Asian Journal of Chemistry; Vol. 33, No. 8 (2021), 1709-1717

ASIAN JOURNAL OF CHEMISTRY

https://doi.org/10.14233/ajchem.2021.23178

Study of Photophysico-chemical and Antimicrobial Photodynamic Properties of Visible Light Active Azometal(II) Complexes

H.B. Teja[1], H.S. Bhojya Naik[1,*], P.H. Amith Nayak[1] and M.C. Prabhakara[2]

[1]Department of P.G. Studies and Research in Industrial Chemistry, School of Chemical Science, Kuvempu University, Shankaragatta-577451, India

[2]Department of P.G. Studies and Research in Industrial Chemistry, Sir M.V. Government Science College, Bommanakatte, Bhadravathi-577302, India

*Corresponding author: E-mail: hsb_naik@rediffmail.com

Received: 22 February 2021; *Accepted*: 5 April 2021; *Published online*: 26 July 2021; AJC-20417

The Co(II) and Mn(II) complexes with octahedral geometries of the type $[Co(L)_2(H_2O)_2]$ and $[Mn(L)_2(H_2O)_2]$ were synthesized and characterized by elemental analysis, FT-IR, UV-visible spectra, powered XRD and photoluminescence. Both metal(II) complexes were prepared with 4-[(*Z*)-(8-hydroxyquinolin-5-yl)diazenyl]-1,5-dimethyl-2-phenyl-1,2-dihydro-3*H*-pyrazol-3-one. The complexes were evaluated for *in vitro* antimicrobial photodynamic activity against Gram-positive, Gram-negative bacteria and fungi. The cell inhibition rate was found to be 80-96%. *in vitro* Cytotoxic studies were performed for the synthesized complexes against human melanoma (A-375) and human primary glioblastoma (U-87) cell lines by MTT assay where Co(II) complex showed potential inhibitory efficiency with IC_{50} value of 115 µg/mL when compared to Mn(II) complex.

Keywords: Metal (II) Complexes, Azo dye, Photosensitizer, Advance photodynamic therapy, Anticancer activity.

INTRODUCTION

Photodynamic therapy is a innovative cancer treatment which includes the irradiation of light with appropriate wavelength, specific photosensitizers can produce reactive oxygen species (ROS). The ROS can produce toxic cytotoxicity that can inactivate the tumour cells [1-3]. Light in combination with a photosensitizer as used to persuade a phototoxic reaction to destroy antibiotic-resistant bacteria [4]. The alternative to treat localized infection is photodynamic therapy [5]. So, photodynamic antimicrobial chemotherapy signifies an alternate antimicrobial treatment against drug resistant organisms [6]. Advance photodynamic therapy has been progressively emerging over the last decades and the demand for novel photosensitizers, including non-porphyrins, phthalocyanines and some macrocyclic systems is still growing [7-9].

Now a days, the development of photosensitizers by using organic dyes is growing in research field, because the organic dye has several advantages such as the effortlessness synthesis, handling, hydrophobicity [10]. To develop environmental friendly, safer and more efficient photosensitizers for antimicrobial photodynamic therapy is a challenge for the researchers. But the efficacy of dye is still relatively low when compared to their inorganic counterparts, which may be due to the highly bonded nature of the electrons in the metal-free organic materials [11]. So, we design the photosensitizers in which the aromatic peripheral ligands around the heavy central metal make it possible to design transition metal complexes [12]. Additionally, the derivatives of 4-aminoantipyrine compounds are applicable as potential ligands for numerous metal complexes having great significance in the field of biochemistry [13]. On the other side, quinoline and related heterocyclic systems are found in a large number of biologically active natural products and pharmaceuticals [14-16]. The nitrogen containing metal complexes deserve a massive significance, because it as ability to break DNA chains and protein [17]. Our interest is to develop a transition metal complexes of organic dye as a binder considering the biocompatibility of both the metal and the ligands, herein, we present the synthesis and characterization of a azo base ligand 4-[(*E*)-(8-hydroxyquinolin-5-yl)diazenyl]-1,5-dimethyl-2-

phenyl-1,2-dihydro-3*H*-pyrazol-3-one and its Co(II) and Mn(II) complexes. The metal(II) complexes structures were conjecture by thermal and electronic spectral data. Furthermore, the cytotoxicity was tested against human melanoma (A-375) and human primary glioblastoma (U-87) cell lines and *in vitro* antimicrobial photodynamic therapy toward Gram-positive bacteria *Staphylococcus aureus*, negative bacteria *Escherichia coli* and fungus *Candida albicans* were also investigated.

EXPERIMENTAL

4-Aminoantipyrine (97%), 8-hydroxy quinoline (98%), sodium nitrate (98%) were purchased from Sigma-Aldrich. Cobalt(II) chloride pentahydrate (97%), magnesium(II) acetate pentahydrate (97%) were purchased from Hi-media and solvents were distilled before use. All other reagents were purchased from Sigma-Aldrich chemicals and were used without further purification. The elemental analyses (C,H,N) were performed by using Perkin-Elmer 2400. Solid-state infrared spectra were recorded with a Thermo Nicolet Avatar IR spectrophotometer using KBr pellets. ^{1}H & ^{13}C NMR spectra were recorded with Bruker 400 MHz high resolution multinuclear FT NMR spectrometer using DMSO as a solvent and TMS as an internal reference. The photoabsorption measurement of complexes were analyzed by Shimadzu model 1650 UV-visible double beam spectrometer in DMF solution (10^{-3} M). The photoluminescence (PL) measurement was performed on Horiba Jobin Yvon Fluorolog-3 equipped with a 450 W Xenon lamp as an excitation source. The thermal analyzer was recorded as TG-DSC curves at a temperature ranging 30-800 ºC in flowing nitrogen atmosphere with a heating rate of 10 ºC/min. The surface morphology of the synthesized compounds were determined by Zeiss scanning electron microscope.

Synthesis of azo-dye: 4-Aminoantipyrine (0.1 mol) was dissolved in 10% HCl and then cooled at 0 to 5 ºC. The $NaNO_2$ (0.1 mol) dissolved in 10 mL of water was added gradually to HCl mixture for 10 min. The reaction mixture was stirred for about 1 h were the temperature was maintained at 0 to 5 ºC. The excess of nitrous acid was removed through the addition of urea, then stirred for about 30 min. The resulting diazonium salt solution was then added dropwise to a well-cooled solution of 8-hydroxyquinoline (0.1 mol) in KOH (5% in 20 mL water) and the pH was maintained at 4-6 by adding Na_2CO_3 under continuous stirring for about 3 h at 0-5 ºC then this precipitated product was diluted with cold water (50 mL). The progress of the reaction was monitored by TLC and then crude dyes were filtered, washed with water and purified by recrystallization from DMF-ethanol (**Scheme-I**) [18]. Yield: 86%; m.p.: 240-242 ºC. Anal. of $C_{20}H_{17}N_5O_2$ calcd. (found) (%): C, 66.84 (66.82); H, 4.77 (4.78); N, 19.49 (19.48); O, 8.90 (8.92). LC-MS (*m/z*) 360.12. IR (KBr, ν_{max}, cm^{-1}): 1634 (C=O), 3422 (OH), 1492 (N=N), 1398 (C-N); ^{1}H NMR (DMSO-d_6, 400 MHz, δ ppm): 11.97 (s, N-H, 2H), 8.67 (s, Ar CH-N), 7.13–8.39 (m, Ar-10H). UV-vis in DMF: 400 nm.

Synthesis of photoreactive Co(II) and Mn(II) complexes: A solution of metal(II) acetate [M = Co^{2+} or Mn^{2+}] (0.005 mol) was taken in 20 mL of absolute ethanol and added dropwise to a stirred solution of 0.01 mol of 4-[(*E*)-(8-hydroxyquinolin-5-yl)diazenyl]-1,5-dimethyl-2-phenyl-1,2-dihydro-3*H*-pyrazol-3-one (**Scheme-II**). The reaction mixture was then refluxed for about 2 h at 70 ºC and then concentrated by heating

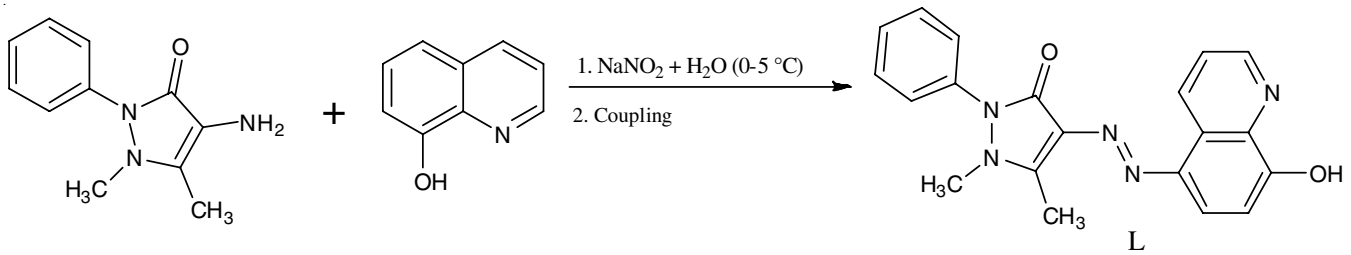

Scheme-I: Synthesis of azo dye ligand (L)

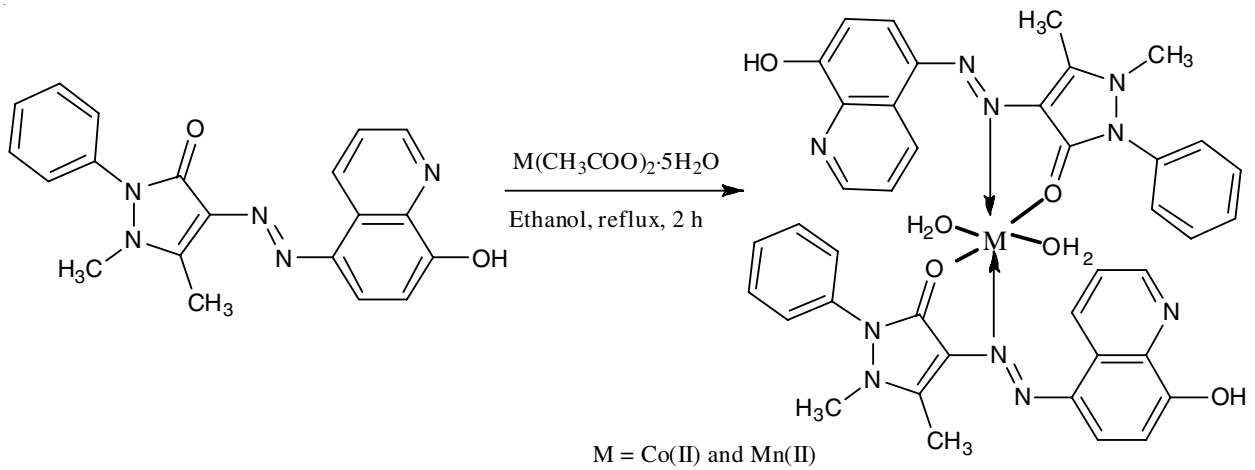

Scheme-II: Metal complexes synthesis by using ligand L

to reduce its volume to half. The precipitate obtained was filtered, washed with hot ethanol and finally dried under vacuum.

Photoinactivation on planktonic cells: From previous report [19], planktonic cells of *E. coli*, *S. aureus* and *C. albicans* was analyzed. An overnight bacterial suspension (100 µL) with a 0.5 McFarland standard containing 1.5×10^8 CFU/mL of bacteria and 1.5×10^7 CFU/mL fungi was transferred to 96 well multitier plates. Test cultures were then treated with photosensitizer of different concentration (20, 40, 60, 80, 100, 150, 200 µg/mL). Photosensitizers were prepared by using non-toxic concentration of DMSO. The samples were pre-incubated for about 3 h in dark condition and subjected to light exposure with xenon lamp of wavelength 400-800 nm for about 15 min irradiated in the presence of foil-cover [20]. The control cultures, with absence of metal(II) complex, were also induced for the same period. The irradiated samples were serially diluted in LB broth and incubated at 37 ºC for 24 h. The reduction in the planktonic cells was calculated by measuring the optical density at 560 nm and stated as percentage reduction by comparing with the OD values of control [21].

***in vitro* Antitumor activity:** Human melanoma (A-375) and human primary glioblastoma (U-87) were used as cell lines to test the cytotoxicity of the metal complexes under study using the reported MTT assay method [22,23]. The cell pellets were maintained in DMEM-HG, the cells were grown in 96 well tissue culture plates. The metal complex of different concentration (50, 100, 150, 200 and 250 µg/mL) and cisplatin the final volume of 200 µL were treated with selected cell lines for about 24 h. After incubation 20 µL of MTT reagent 0.5 mg/mL concentration was added to each well and incubated for further 3 h. The medium was replaced with DMSO (100 µL/well) to dissolve the formazan crystals. The effects of the different test compounds on the viability of the tumor cell lines were measured at 540 nm using a multimode reader. All samples (five concentrations of each sample) were tested in triplicate and using origin software, IC_{50} values with standard deviation were calculated [24].

***in silico* Molecular docking studies:** The crystal structure of RSCB with PDB id 4NNI was obtained from the protein data bank (PDB) and used as a receptor for RpsA protein in complex with standard pyrazinoic acid (POA). The obtained file was utilized for *in silico* molecular docking of protein with metal(II) complexes using Autodock 4.2. The structures of the studied compounds were developed using Chem Bio Office Ultra 14.0 software assigned with proper three-dimensional orientation followed by the minimization of energy based on Lamarckian genetic algorithm. The performance of docking of receptor (DNA) and ligand (complex) was based on the glide energy, docking score was analyzed by the active site hydrogen bonds and hydrophobic interactions. Finally, according to the Autodocking scores was used to obtain the best conformation energy [25,26].

RESULTS AND DISCUSSION

The synthesis of visible light active azometal(II) complexes was based on the fact that the electrophilic aromatic diazonium ions reacts with the nucleophilic activated aromatics at 0 ºC. The azometal(II) complexes were characterized using LC-MS, ^{1}H & ^{13}C NMR, FTIR and UV-VIS spectroscopic and elemental analyses. The obained results are consistent with the structure. The azo dyes was then reacted with metal salts to form octahedral azo metal complexes. The physico-analytical data of the ligand L and its metal(II) complexes are presented in Table-1. Using TGA-DSC, photoluminescence and FT-IR studies the formation of metal complexes were conformed.

Photodynamic therapy with synthesized metal complexes at high concentration promotes a significant reduction in the number of CFU mL^{-1} of bacteria and fungi. No toxicity was found for the cells irradiated without photosensitizers, the cell death of microbial cells was not affected by irradiation without photosensitizer, thus the photoinactivation of microorganisms depends on both concentration of the photosensitizers and the irradiation time.

^{1}H & ^{13}C NMR spectra: ^{1}H NMR spectra of the synthesized ligand obtained at ambient temperature in DMSO-d_6, displayed signals at δ 9.06-9.08 (doublet), which corresponds to -N-CH- of the quinoline ring [27]. The signal at δ 8.89 ppm was assigned to -OH group of 8-hydroxyquinoline ring and this downfield shift was due to the intramolecular hydrogen bonding between -OH of 8-hydroxyquinoline ring [28]. The aromatic protons showed a signal at δ 7.3-7.7 ppm as a multiplet [29]. A sharp singlet at δ 3.34 and δ 2.68 ppm were assigned to the methyl protons of 4-aminoantipyrine moiety [30].

^{13}C NMR of azo dye displayed a signal at δ 151 ppm, which attributes to -N-CH of the quinoline ring. Signal at δ 155.5 ppm corresponds to carbon attached to the -OH of 8-hydroxyquinoline [29] Signals at δ 111 and 122 ppm were assigned to the adjacent carbon atom of the azo group. The methyl carbon of the antipyrine were assigned at δ 34 ppm (-N-CH_3) and δ 11 ppm (-C-CH_3) [31].

Mass spectra: The mass spectra of the ligand exhibited a well-defined molecular ion peak at *m/z* = 359 molecular ion (parent peak), peak at 360 *m/z* was due to (M+1). The fragment appeared at *m/z* = 241 corresponds to the fragment of [$C_{13}H_{13}N_4O$], which indicates the formation of azo compound [32].

FTIR spectra: The main characteristic bands and their tentative frequencies are summarized in Table-2. The strong IR band at 1634 cm^{-1} in the free ligand was assigned to the

TABLE-1
PHYSICAL DATA OF THE SYNTHESIZED COMPOUNDS

Synthesized compound	m.w.	Yield (%)	m.p. (°C)	Solubility	Elemental analysis (%): Found (calcd.)				
					C	H	N	O	M
$L(C_{19}H_{15}N_5O_2)$	359.14	80	258-260	DMSO/DMF	67.00 (66.84)	4.64 (4.77)	19.50 (19.49)	8.880 (8.90)	–
$Co(L)_2(H_2O)_2$	872.16	75	> 300	DMSO/DMF	55.00 (55.05)	4.42 (4.39)	16.11 (16.05)	11.042 (11.0)	13.61 (13.51)
$Mn(L)_2(H_2O)_2$	864.17	60	> 300	DMSO/DMF	55.49 (55.56)	4.32 (4.43)	16.16 (16.20)	11.089 (11.10)	12.80 (12.71)

TABLE-2
FT-IR BANDS (cm^{-1}) AND TENTATIVE ASSIGNMENTS OF THE LIGAND AND ITS METAL AZO COMPLEXES

Compounds	ν(–OH)	ν(C=O)	ν(N=N)	ν(M–N)	ν(M–O)
L	3422	1634	1492	–	–
$Co(L)_2(H_2O)_2$	3377	1563	1458	488	693
$Mn(L)_2(H_2O)_2$	3390	1563	1461	443	515

stretching of carbonyl group present in 4-aminoantipyrine moiety. In the spectra of complexes [33], these bands shifted significantly towards lower energy, which indicates a decrease in the stretching force of (-C=O). As a result, coordination occurs through the carbonyl oxygen atoms [34]. The stretching frequency at 1492 cm^{-1} corresponds to the azo group (-N=N-), this band also shifted towards lower energy in the complexes. It shows that the one of the nitrogens in azo group was involved in the complex formation. In the ligand, a broad peak at 3422 cm^{-1} corresponds to –OH of the quinoline ring since the –OH group involved in inter or intra molecular hydrogen bonding. Khoo *et al.* [35] suggested that stable azo form is due to inter molecular hydrogen bonding at solid state. The broad peak at 3400-3350 cm^{-1} presents in both complexes attributes to the presence of water molecule in the coordination with the metal ions. The presence of water in these complexes was also confirmed by thermal analysis. The presence of new band in metal complexes at 693-488 and 618-483 cm^{-1} assigned to M–N of the azo nitrogen and M–O of the antipyrine moiety, respectively [36].

Electronic spectra: The electronic absorption spectra in the UV-visible region for the ligand precursor, as well as their corresponding complexes, were recorded in DMF solution. The absorbtion of the free ligand was at 24509 cm^{-1} arises due to the transition involving electron migration along the entire conjugate system of the ligand. The bathocromic shift was observed in metal(II) azo complexes related to their free azo ligand (Fig. 1), which shows that the metal(II) complexes showed red shift of 4 nm when compared to that of free ligand [37]. According to molecular orbital theory, the center metal(II) ions have influence on the absorption bands of the complexes. The metal complexes exhibited new bands in the range of 20400-20000 cm^{-1} assigned to charge transfer spectrum (LMCT), which were absent in ligand [38]. The cobalt(II) complex showed

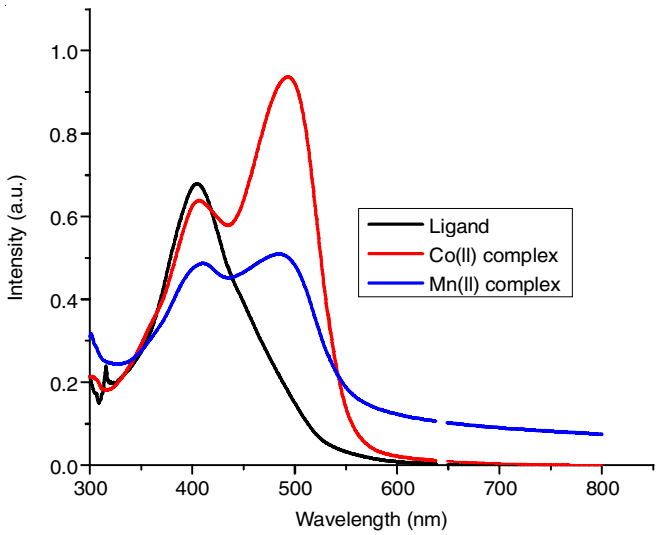

Fig. 1. UV-visible spectra of the ligand (L) and metal complexes

the absorption of 24619 and 20325 cm^{-1} and the bands were assigned as $^4T_{1g}(F) \rightarrow {}^4T_{2g}(F)$ and $^4T_{1g}(F) \rightarrow {}^4A_{2g}(F)$, which showed a distorted octahedral geometry [39]. The spectrum of the octahedral Mn(II) complex shows two bands at 24330 and 20242 cm^{-1} due to $^6A_{1g} \rightarrow {}^4T_{1g}$ and $^6A_{1g} \rightarrow {}^4T_{2g}$ transitions. Mn(II) complex has ground state $^6A_{1g}$, hence the transition from this ground state $^6A_{1g} \rightarrow {}^4E$ (d) is forbidden and band intensity was very low [40].

Thermal studies: Thermal properties of metal(II) complexes were investigated by thermogravimetric (TG) analysis and differential scanning calorimetry (DSC) in the temperature range of 30-800 ºC in nitrogen atmosphere and the weight loss was observed in room temperature. Generally, the thermogram showed three stages of decomposition (Fig. 2). The first

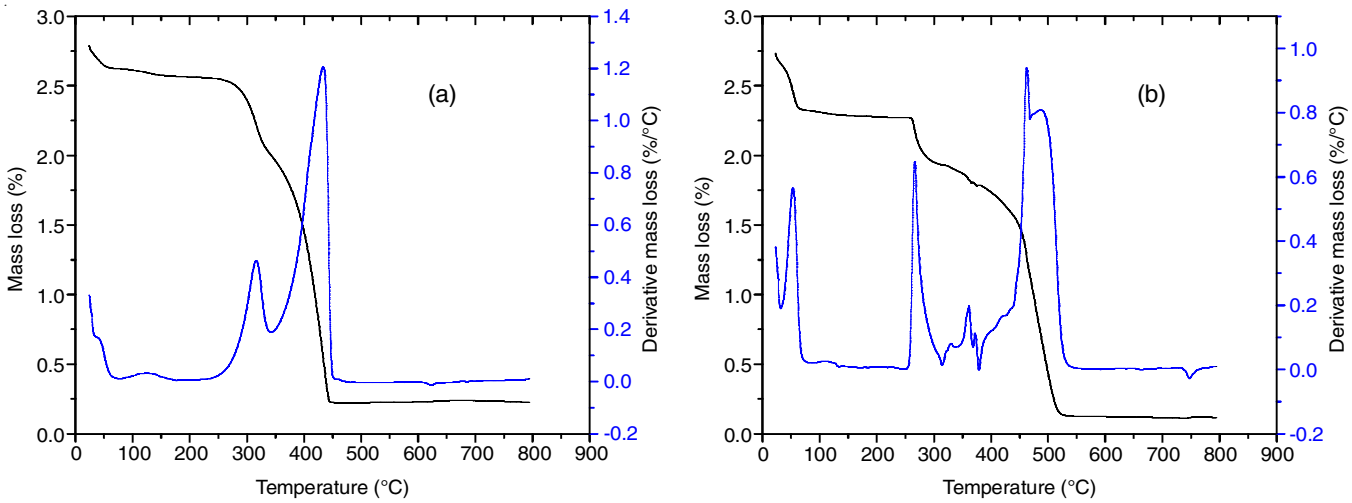

Fig. 2. TG/DSC curve of (a) $Co(L)_2(H_2O)_2$ (b) $Mn(L)_2(H_2O)_2$

step attributed to the loss of coordinated solvent molecules, in the temperature range of 40-120 ºC, for Co(II) complex it corresponds to the strong water molecule, where as in Mn(II) it correlate with weakly coordinated water molecule (Table-3). In second stage, at ~320 ºC the peak intimates the dissociation of non-coordinated quinolin-8-ol group. In third step, the loss of aminophenazone moiety attributed at ~450 ºC, probably was due to the intermolecular π-interation. Further, heating resulted in continuous loss of mass, indicating the decomposition of the molecules, which was not complete up to 800 ºC due to the presence of metal oxide. The overall dissociation was found to be ~93%.

SEM images: Scanning electron micrograph (SEM) have been used to study the morphology and the grain size of the ligand and the metal(II) complexes. The SEM photographs of the complexes are shown in Fig. 3, which were taken in different scale ranges from 10 µm to 100 µm. The SEM photography of the ligand demonstrated non-uniform platelet-like structure with variable lateral dimensions [41]. For Co(II) complex, a niddle shaped structure was observed while the irregular shaped grains were seen in Mn(II) complexs.

XRD studies: The degree of crystallinity of the synthesis metal complexes was studies by using powdered XRD by using polar solvents like DMSO and DMF. The X-ray diffractogram of metal(II) complexes were obtained in the range of 10-80º (2θ) at a wavelength of 1.54 Å. The XRD patterns of both metal(II) complexes are depicted in Fig. 4. The XRD patterns of Co(II) and Mn(II) complexes shows 10 and 9 reflection in the range 9 to 40º (2θ). The inter planar spacing were calculated by means of Bragg's equation $n\lambda = 2d \sin\theta$ (where $\lambda = 1.5406$

TABLE-3
THERMAL DECOMPOSITION OF THE METAL COMPLEXES AT NITROGEN

Complexes	Stages	Temp. range (°C)	Dsc peak	Peak nature	Mass loss (%): Found (calcd.)	Probable assignments	Residue
$Co(L)_2(H_2O)_2$	Stage 1	34-110	114.8	endo	6.46 (6.52)	Loss of $2H_2O$	CoO
	Stage 2	111-370	317	exo	34.67 (35.02)	Loss of $C_{18}H_{14}N_2O_2$	
	Stage 3	370-440	434	exo	53.4 (52.18)	Loss of $C_{22}H_{24}N_8O_2$	
$Mn(L)_2(H_2O)_2$	Stage 1	47-90	54	exo	6.47 (6.53)	Loss of $2H_2O$	MnO
	Stage 2	91-390	266	exo	36.7 (35.081)	Loss of $C_{18}H_{14}N_2O_2$	
	Stage 3	390-450	361	endo	51.4 (52.23)	Loss of $C_{22}H_{24}N_8O_2$	
			461	exo			

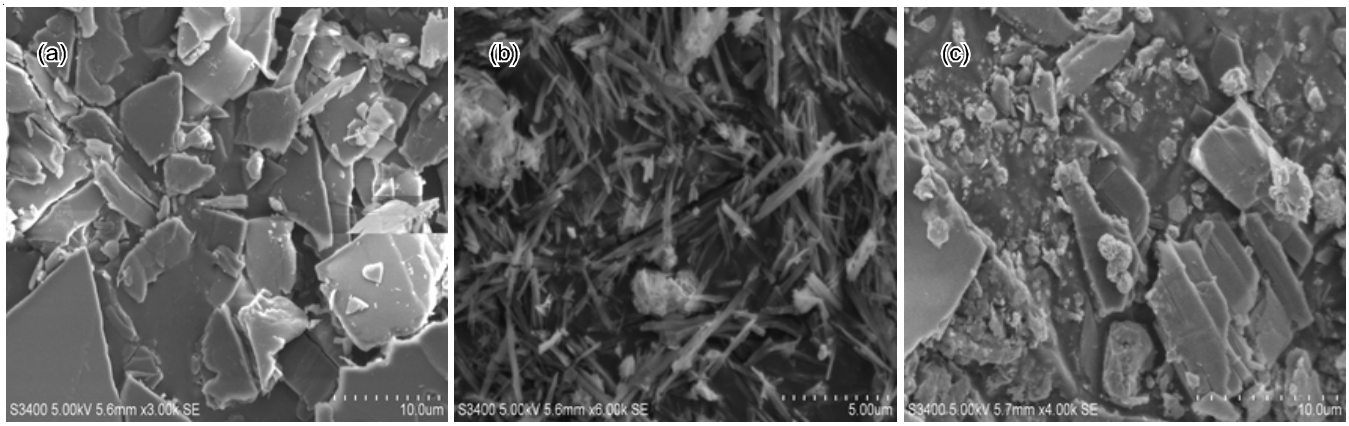

Fig. 3. SEM image of (a) Ligand, (b) $Co(L)_2(H_2O)_2$ (c) $Mn(L)_2(H_2O)_2$

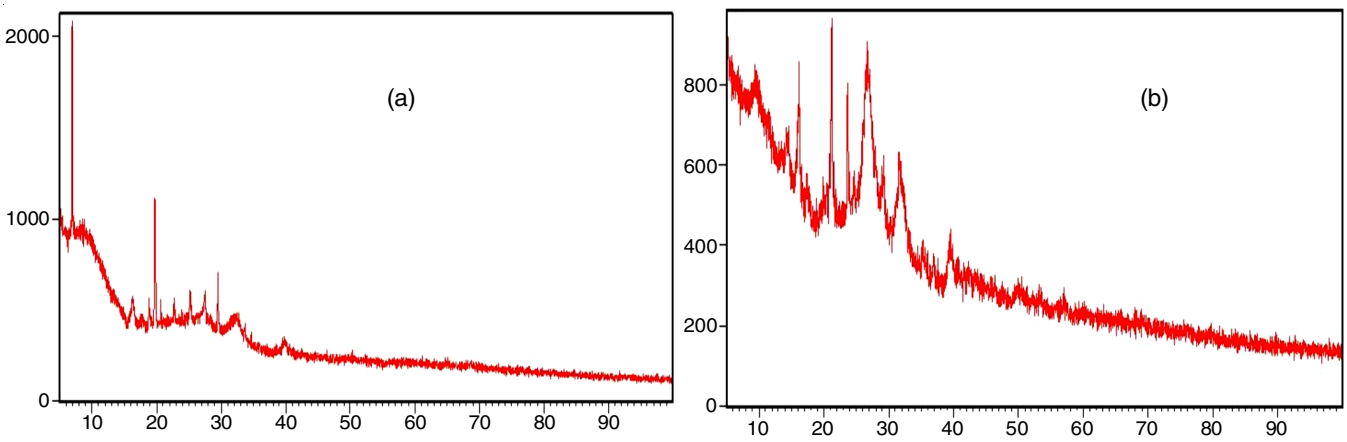

Fig. 4. Powder XRD data for metal complexes (a) $Co(L)_2(H_2O)_2$ (b) $Mn(L)_2(H_2O)_2$

Å). The obtained and calculated *d*-spacing values were found to be in good agreement (Table-4).

The unit cell calculations were calculated for cubic symmetry by all the obtained peaks, miller indices (h k l) values were determined. The $h^2 + k^2 + l^2$ values of Co(II) 1, 6, 7, 8, 11, 13, 16. For Mn(II) was found to be 1, 3, 8, 10, 11, 15, 17, 21, 22. The calculated lattice parameter for Co(II) complex found to be $a = b = c = 12.8$ Å and for Mn(II) complex $a = b = c =$ 17.1 Å. The existence of forbidden number 7 for Co(II) and 15 for Mn(II) indicates that complexes may belong to hexagonal or tetragonal systems.

Photoluminescence spectra: Photoluminescence spectra of ligand and its azo metal(II) complexes were recorded in room temperature. The samples were excited by single excitation wavelength of 400 nm with the excitation source of 450 W Xenon lamp as shown in Fig. 5. The emission spectra of the ligand showed the excitation at 400 nm. The free azo dye ligand exhibited intra ligand π-π* transitions. The emission spectrum of Co(II) showed strong emission peck at 530 nm at the excitation of 400 nm. But Mn(II) complex showed the emission peak at 700 nm at the excitation of 400 nm. The decreased intensity of Mn(II) complex may be due to the formation of metal complexes and the energy transferes from the excited ligand to the metal ion [42]. The significant difference in position and intensity of the metal complexes shows the coordination of the metal ion to the peripheral ligand [43]. In general, all the synthesized compounds can serve as potential photoactive materials as indicated from their characteristic photoluminescence property.

TABLE-4
POWDERED XRD DATA OF METAL COMPLEXES (a) $Co(L)_2(H_2O)_2$ and (b) $Mn(L)_2(H_2O)_2$

Peak number	2θ	θ	sin θ	$\sin^2\theta$	1000 $\sin^2\theta$	$h^2 + k^2 + l^2$ (1000 $\sin^2\theta$/CF)	*h k l*	D		a (Å)
								Obs.	Calcd.	
(a) $Co(L)_2(H_2O)_2$										
1	6.9057	3.452	0.0602	0.003625	3.625	1(1)	100	12.793	12.800	12.79
2	16.2760	8.138	0.1415	0.02003	20.03	5.52(6)	211	5.441	5.446	13.33
3	18.8127	9.406	0.1630	0.02671	26.71	7.36(7)	–	4.713	4.717	12.46
4	19.6690	9.834	0.1708	0.02917	29.17	8.04(8)	220	4.510	4.513	12.75
5	22.7479	11.373	0.1972	0.03888	38.88	10.72(11)	311	3.906	3.909	12.95
6	25.7479	12.593	0.2180	0.04753	47.53	13.11(13)	320	3.533	3.235	12.73
7	27.4482	13.724	0.2372	0.05628	56.28	15.52(16)	400	3.246	3.249	12.98
8	29.4582	14.729	0.2542	0.06464	64.64	17.83(18)	411	3.029	3.032	12.85
9	32.6210	16.310	0.2808	0.07887	78.87	21.75(22)	332	2.742	2.745	12.86
(b) $Mn(L)_2(H_2O)_2$										
1	5.1632	2.5816	0.0450	0.00202	2.028	1(1)	100	17.101	17.116	17.10
2	9.3787	4.6893	0.0817	0.00668	6.683	3.29(3)	111	9.422	9.422	16.31
3	14.3955	7.1977	0.1252	0.01569	15.69	7.74(8)	220	6.147	6.153	17.39
4	16.1954	8.0976	0.1408	0.01984	19.84	9.78(10)	310	5.468	5.473	17.29
5	17.3696	8.6848	0.1509	0.02280	22.80	11.24(11)	311	5.101	5.105	16.91
6	19.9378	9.9689	0.1731	0.02996	29.96	14.77(15)	---	4.449	4.449	17.23
7	21.2131	10.6068	0.1840	0.03388	33.88	16.70(17)	410	4.184	4.188	17.25
8	23.6635	11.8317	0.2050	0.04204	42.04	20.72(21)	421	3.756	3.759	17.21
9	24.6174	12.3087	0.2131	0.04544	45.44	22.40(22)	332	3.613	3.613	16.94

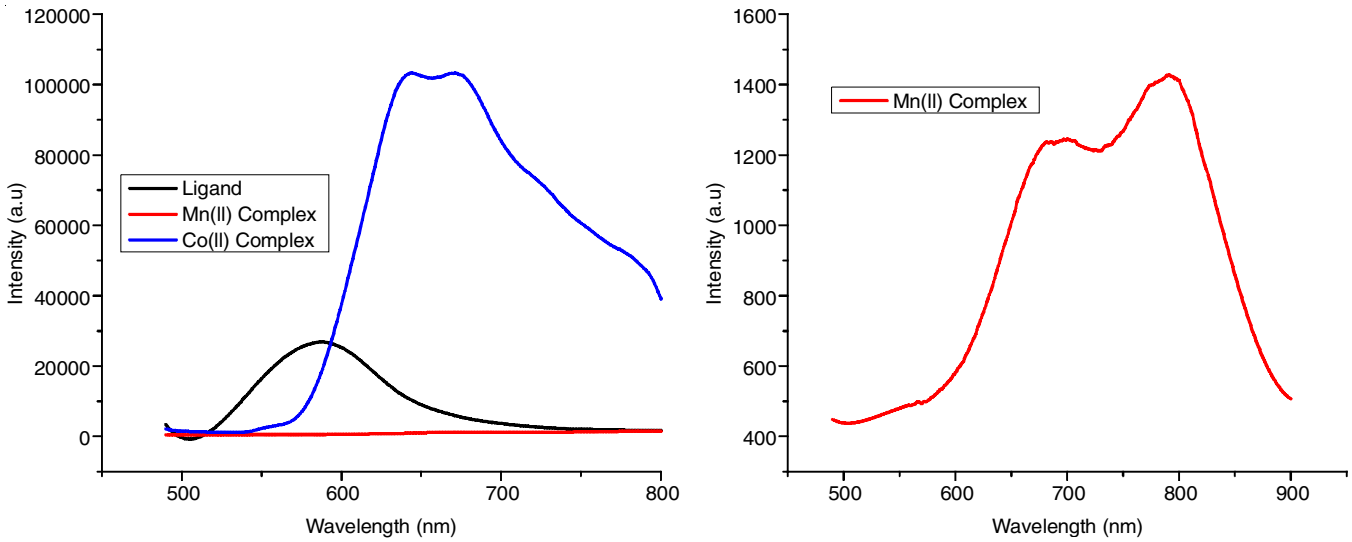

Fig. 5. Photoluminescence spectra of the ligand and its metal complexes

Biological applications

***in vitro* Antimicrobial studies:** The results of this demonstrated that photosensitizers with xenon lamp at the concentration of 200 µg/mL showed significant reduction in plantonic cells when compared to methylene blue (MB). To the best of our knowledge, this is the first study in the literature reporting the plantonic effect of Co(II) and Mn(II) complexes on bacteria as well as fungi. The antimicrobial photodynamic therapy is an effective process in presence of light. Based on these results, order of susceptibility of bacteria towards photolysis in presence of Co(II) and Mn(II) complex is given as: *S. aureus* > *E. coli* > *C. albicans*.

In this work, the cell reduction % of *S. aureus* were plotted against the concentration. The interaction of *S. aureus* with metal photosensitizers is shown in Fig. 6a. The percentage inhibition of Co(II) and Mn(II) complex was 96% and 84%, respectively. Fig. 6b shows the photoinhibition of *E. coli* were the inhibition rate was found to be 82% and 78%. Comparing the inactivation of bacterias, Gram-negative bacteria was more resistance than Gram-positive bacteria, due to the structural difference of the Gram-negative bacteria and the presence of an additional and more negatively charged outer layer, serves as a barrier to prevent the entry of outer species. The percentage inhibition of *S. aureus* of Co(II) complex was high when compared to Mn(II) complex which may due to the high abortion in fluorescence, the photons will not have sufficient energy for the ground state oxygen molecule to excite the singlet oxygen and shorter wavelength leads to less tissue penetration and more likely leads to skin photosensitivity [44]. The photoinactivation of *C. albicans* is shown in Fig. 6c. The cell death rate was absorbed to be 74 and 70% for fungi where the percentage death was decreased compared to bacteria. Also, the antifungal advance photodynamic therapy (APDT) involves more complex mechanisms [45].

For both metal complexes, the concentration dependents on the growth inhibition as observed. As the concentration was increased the growth inhibition also increased. High reduction of plantonic cells at higher concentration was observed. This is because of self-shielding of the photosensitizer, molecules will absorbs the light at top of the sample, which will prevent the light penetration through the sample and activation of the photosensitizer below it leads to the generation of ROS at aproximal location to the targeted bacteria [46].

***in vitro* Antitumor activity:** *in vitro* Antiproliferative studies of metal complexes were analyzed against two tumour cell lines using MTT assay, which was used extensively for *in vitro* cytotoxic studies [45]. Different concentrations of complexes (50, 100, 150, 200 and 250 µg/mL) were treated with the tumour cell lines and clinical drug cisplatin was used as a control. The metal complexes inhibited the growth of cancer cells with the increase in concentration of the drug. At higher concentration, Co(II) and Mn(II) complexes cell viability of human melanoma (A-375) were found to be 16.84% and 21.4%, for human primary glioblastoma (U-87) 8.75% and 26% clearly indicate that the complexes have caused the death of most of the tumor cells at this concentration. The IC_{50} values and cell viability data are given in Table-5.

TABLE-5
IC_{50} VALUES OF AZO METAL COMPLEXES ON A-375 AND U-78 CANCER CELLS

Compound	A-375 (IC_{50})	Inhibition (%)	U-78 (IC_{50})	Inhibition (%)
$Co(L)_2(H_2O)_2$	74	92	115	84
$Mn(L)_2(H_2O)_2$	50.5	74	42	64

The synthesized compound shows good cytotoxic activity but lesser activity when compared to standard drug (Fig. 7). Also Co(II) complex shows better activity than Mn(II) complex. This selectivity may be explained based on the mode of action of cobalt complex. The cobalt(II) ions are able to induce in the formation of ROS in physiological conditions, thus the increase of ROS levels leads to oxidative macromolecular damage and elimination of cancer cells. For metal(II) complex, the IC_{50} value was more than 100 indicated that the complex probably was non-toxic in nature [47].

***in silico* Molecular docking studies:** All the synthesized metal complexes were employed to understand the interaction between the metal complexes with the target receptor molecules (RpsA) [48]. The binding sites of complexes (**1-2**) on DNA are shown in Fig. 8. All the synthesized complexes have the capacity to interrelate with DNA through a small groove. The binding energies of the complexes (**1-2**) are presented in Table-5. The Co(II) complex shows the highest binding energy of -3.55 and showed good interactions with the DNA.

Conclusion

In conclusion, a series of novel photosensitizers based on 8-hydroxy quinoline derivatives were synthesized and their photophysical and photochemical properties were investigated. The spectral studies suggested that the ligand was coordinated

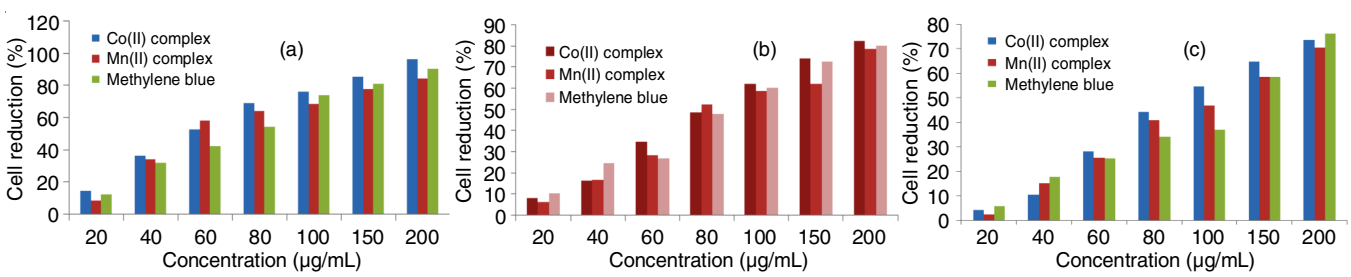

Fig. 6. Relative cell reduction of three strains (a) *S. aureus*, (b) *E. coli* and (c) *C. albicans* after being irradiated with laser for 15 min and then incubated with photosensitizers and methylene blue

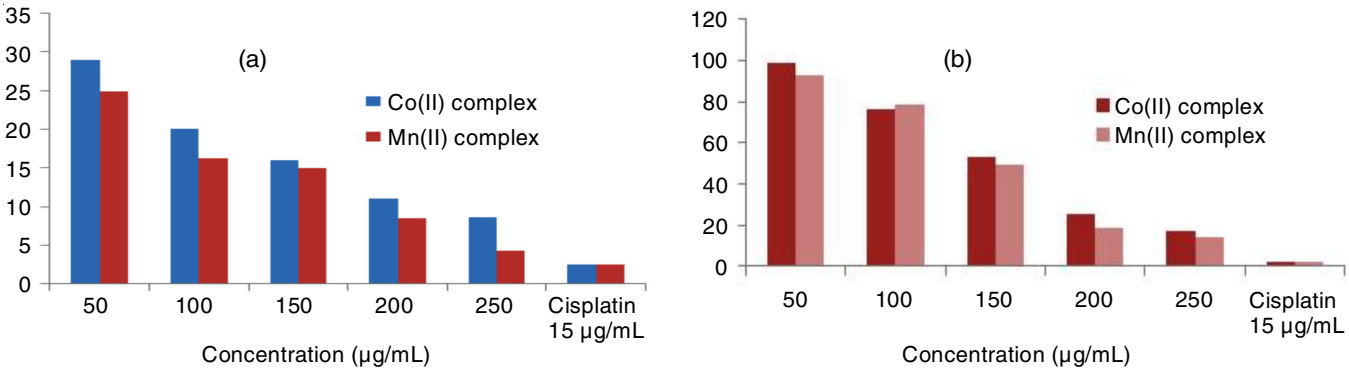

Fig. 7. Cytotoxicity activity of metal complex with (a) U-87 cell line and (b) A-378 cell line

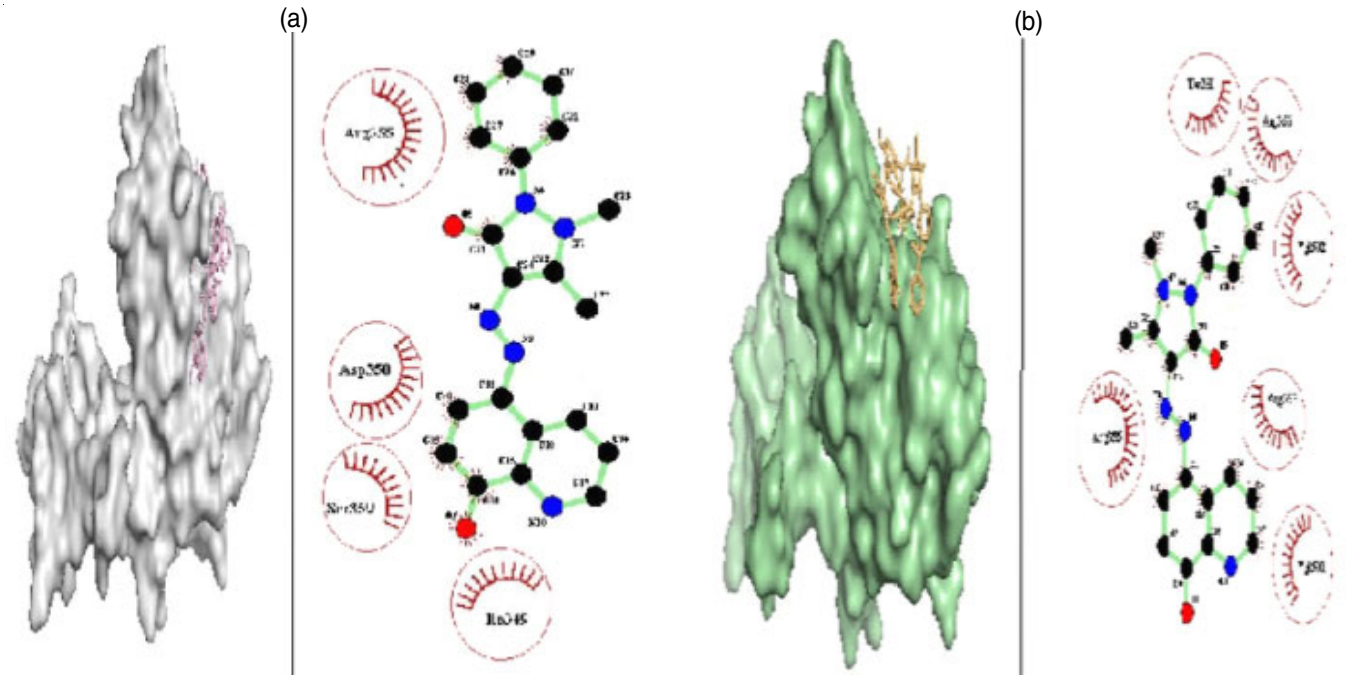

Fig. 8. Three-dimensional molecular docking displaying (a) $Co(L)_2(H_2O)_2$ (b) $Mn(L)_2(H_2O)_2$

with the metal ion through the oxygen of 4-aminoantipyrine and the nitrogen of azo group with the octahedral geometry. The thermal data demonstrate the presence of water molecule in the complexes. The synthesized complexes were evaluated for cytotoxicity and APDT studies. Both complexes showed the cytotoxic activity, but cobalt(II) complex was more active towards human melanoma cell line. The antimicrobial photodynamic activity of *S. aureus*, *E. coli* and fungus *C. albicans* was also tested. The highest cell reduction was found to be 96% in *S. aureus* at a concentration of 200 µg/mL. The effective binding interactions between the tested compounds and the target receptor RpsA was studied by using *in silico* molecular docking studies. This shows that the metal complexes with azo ligand, proves to be promising candidates as photoactive antimicrobial activity and also alternatives to the anticancer drug.

CONFLICT OF INTEREST

The authors declare that there is no conflict of interests regarding the publication of this article.

REFERENCES

1. Á. Juarranz, P. Jaén, F. Sanz-Rodríguez, J. Cuevas and S. González, *Clin. Transl. Oncol.*, **10**, 148 (2008); https://doi.org/10.1007/s12094-008-0172-2
2. R.R. Allison, H.C. Mota and C.H. Sibata, *Photodiagn. Photodyn. Ther.*, **1**, 263 (2004); https://doi.org/10.1016/S1572-1000(04)00084-5
3. R.R. Allison and C.H. Sibata, *Photodiagn. Photodyn. Ther.*, **7**, 61 (2010); https://doi.org/10.1016/j.pdpdt.2010.02.001
4. L. Cizeková, A. Grolmusová, Z. Ipóthová, Z. Barbieriková, V. Brezová, L. Hunáková, J. Imrich, L. Janovec, I. Dovinová and H. Paulíková, *Bioorg. Med. Chem.*, **22**, 4684 (2014); https://doi.org/10.1016/j.bmc.2014.07.013
5. A. Gasparetto, T.F. Lapinski, S.R. Zamuner, S. Khouri, L.P. Alves, E. Munin and M.J. Salvador, *J. Photochem. Photobiol. B*, **99**, 15 (2010); https://doi.org/10.1016/j.jphotobiol.2010.01.009
6. N. Barbero, S. Visentin and G. Viscardi, *J. Photochem. Photobiol. Chem.*, **299**, 38 (2015); https://doi.org/10.1016/j.jphotochem.2014.11.002
7. A.P. Castano, T.N. Demidova and M.R. Hamblin, *Photodiagn. Photodyn. Ther.*, **1**, 279 (2004); https://doi.org/10.1016/S1572-1000(05)00007-4
8. M.S. Baptista and M. Wainwright, *J. Med. Biol. Res.*, **44**, 1 (2011); https://doi.org/10.1590/S0100-879X2010007500141

9. M. Managa, E.K. Amuhaya and T. Nyokong, *Spectrochim. Acta A Mol. Biomol. Spectrosc.*, **151**, 867 (2015); https://doi.org/10.1016/j.saa.2015.06.088
10. Y.D. Kim, J.H. Cho, C.R. Park, J.-H. Choi, C. Yoon and J.P. Kim, *Dyes Pigments*, **89**, 1 (2011); https://doi.org/10.1016/j.dyepig.2010.07.008
11. V. Kumar, M. Gohain, J.H. Van Tonder, B.C.B. Bezuindenhoudt, S. Ponra, O.M. Ntwaeaborwa and H.C. Swart, *Opt. Mater.*, **50**, 275 (2015); https://doi.org/10.1016/j.optmat.2015.11.009
12. N.C. Warshakoon, J. Sheville, R.T. Bhatt, W. Ji, J.L. Mendez-Andino, K.M. Meyers, N. Kim, J.A. Wos, C. Mitchell, J.L. Paris, B.B. Pinney, O. Reizes and X.E. Hu, *Bioorg. Med. Chem. Lett.*, **16**, 5207 (2006); https://doi.org/10.1016/j.bmcl.2006.07.006
13. R. Teran, R. Guevara, J. Mora, L. Dobronski, O. Barreiro-Costa, T. Beske, J. Pérez-Barrera, R. Araya-Maturana, P. Rojas-Silva, A. Poveda and J. Heredia-Moya, *Molecules*, **24**, 2696 (2019); https://doi.org/10.3390/molecules24152696
14. S. Kumar, S. Bawa and H. Gupta, *Mini Rev. Med. Chem.*, **9**, 1648 (2009); https://doi.org/10.2174/138955709791012247
15. H.-R. Zhang, K.-B. Huang, Z.-F. Chen, Y.-C. Liu, Y.-N. Liu, T. Meng, Q.-P. Qin, B.-Q. Zou and H. Liang, *MedChemComm*, **7**, 806, (2016); https://doi.org/10.1039/C6MD00073H
16. M.C. Prabahkara and H.S. Bhojya Naik, *Biometals*, **21**, 675 (2008); https://doi.org/10.1007/s10534-008-9152-9
17. C.N. Sudhamani, H.S. Bhojya Naik and D. Girija, *Synth. React. Inorg. Met.-Org. Nano-Met. Chem.*, **42**, 518 (2012); https://doi.org/10.1080/15533174.2011.613439
18. M.A. Gouda, H.F. Eldien, M.M. Girges and M.A. Berghot, *J. Saudi Chem. Soc.*, **20**, 151 (2016); https://doi.org/10.1016/j.jscs.2012.06.004
19. C.H. Kim, E.S. Lee, S.M. Kang, E. de Josselin de Jong and B.-I. Kim, *Photodiagn. Photodyn. Ther.*, **18**, 279 (2017); https://doi.org/10.1016/j.pdpdt.2017.03.015
20. A. Vt, P. Paramanantham, S.L. Sb, A. Sharan, M.H. Alsaedi, T.M.S. Dawoud, S. Asad and S. Busi, *Photodiagn. Photodyn. Ther.*, **24**, 300 (2018); https://doi.org/10.1016/j.pdpdt.2018.10.013
21. C.N. Sudhamani, H.S. Bhojya Naik, K.R.S. Gowda, M. Giridhar, D. Girija and P.N.P. Kumar, *Med. Chem. Res.*, **26**, 1160 (2017); https://doi.org/10.1007/s00044-017-1831-z
22. S. Ali, V. Singh, P. Jain and V. Tripathi, *J. Saudi Chem. Soc.*, **23**, 52 (2019); https://doi.org/10.1016/j.jscs.2018.04.005
23. M. Zhu, J. Liu, J. Su, B. Meng, Y. Feng, B. Jia, T. Peng, Z. Qi and E. Gao, *Appl. Organomet. Chem.*, **33**, 4676 (2019); https://doi.org/10.1002/aoc.4676
24. P. Vijayan, P. Viswanathamurthi, K. Velmurugan, R. Nandhakumar, M.D. Balakumaran, P.T. Kalaichelvan and J.G. Malecki, *RSC Adv.*, **5**, 103321 (2015); https://doi.org/10.1039/C5RA18568H
25. A. De, H.P. Ray, P. Jain, H. Kaur and N. Singh, *J. Mol. Struct.*, **1199**, 126901 (2020); https://doi.org/10.1016/j.molstruc.2019.126901
26. A.Y. Al-Dawood, N.M. El -Metwaly and H.A. El-Ghamry, *J. Mol. Liq.*, **220**, 311 (2016); https://doi.org/10.1016/j.molliq.2016.04.079
27. V.A. Mamedov, V.R. Galimullina, N.A. Zhukova, S.F. Kadyrova, E.V. Mironova, I.K. Rizvanov and S.K. Latypov, *Tetrahedron Lett.*, **55**, 4319 (2014); https://doi.org/10.1016/j.tetlet.2014.06.023
28. A. Saylam, Z. Seferoglu and N. Ertan, *J. Mol. Liq.*, **195**, 267 (2014); https://doi.org/10.1016/j.molliq.2014.02.027
29. G. Karpiñska, A.P. Mazurek and J.C. Dobrowolski, *J. Mol. Struct. THEOCHEM*, **961**, 101 (2010); https://doi.org/10.1016/j.theochem.2010.09.006
30. M. Manjunath, A.D. Kulkarni, G.B. Bagihalli, S. Malladi and S.A. Patil, *J. Mol. Struct.*, **1127**, 314 (2016); https://doi.org/10.1016/j.molstruc.2016.07.123
31. N. Venugopal, G. Krishnamurthy, H.S. Bhojyanaik and P. Murali Krishna, *J. Mol. Struct.*, **1183**, 37 (2019); https://doi.org/10.1016/j.molstruc.2019.01.031
32. M.A. Ayoub, *J. Mol. Struct.*, **1173**, 17 (2018); https://doi.org/10.1016/j.molstruc.2018.06.051
33. S.A.F. Rostom, I.M. El-Ashmawy, H.A. Abd El Razik, M.H. Badr and H.M.A. Ashour, *Bioorg. Med. Chem.*, **17**, 882 (2009); https://doi.org/10.1016/j.bmc.2008.11.035
34. X. Li, Y. Wu, D. Gu and F. Gan, *Dyes Pigments*, **86**, 182 (2010); https://doi.org/10.1016/j.dyepig.2010.01.002
35. M.K.B. Break, M. Ibrahim M. Tahir, K.A. Crouse and T.-J. Khoo, *Bioinorg. Chem. Appl.*, **2013**, 362513 (2013); https://doi.org/10.1155/2013/362513
36. S.M. Pradeepa, H.S. Bhojya Naik, B.V. Kumar, K.I. Priyadarsini, A. Barik and M.C. Prabhakara, *Spectrochim. Acta A Mol. Biomol. Spectrosc.*, **141**, 34 (2015); https://doi.org/10.1016/j.saa.2015.01.019
37. S.M. Pradeepa, H.S. Bhojya Naik, B.V. Kumar, K.I. Priyadarsini, A. Barik, T.R. Ravikumar Naik and M.C. Prabhakara, *Spectrochim. Acta A Mol. Biomol. Spectrosc.*, **115**, 12 (2013); https://doi.org/10.1016/j.saa.2013.06.009
38. K. Andiappan, A. Sanmugam, E. Deivanayagam, K. Karuppasamy, H.-S. Kim and D. Vikraman, *Sci. Rep.*, **8**, 3054 (2018); https://doi.org/10.1038/s41598-018-21366-1
39. T. Manjuraj, G. Krishnamurthy, Y.D. Bodke, H.S.B. Naik and H.S. Anil Kumar, *J. Mol. Struct.*, **1171**, 481 (2018); https://doi.org/10.1016/j.molstruc.2018.06.055
40. M. Sennappan, P.M. Krishna, R. Ranganathan and P. Sivakami Sundari, *J. Mol. Struct.*, **1179**, 86 (2019); https://doi.org/10.1016/j.molstruc.2018.10.087
41. N.K. Chaudhary and P. Mishra, *Bioinorg. Chem. Appl.*, **2017**, 6927675 (2017); https://doi.org/10.1155/2017/6927675
42. O.A.M. Ali, S.M. El-Medani, D.A. Ahmed and D.A. Nassar, *Spectrochim. Acta A Mol. Biomol. Spectrosc.*, **144**, 99 (2015); https://doi.org/10.1016/j.saa.2015.02.078
43. Z. Sun, S. Zhou, H. Qiu, Y. Gu and Y. Zhao, *RSC Adv.*, **8**, 17073 (2018); https://doi.org/10.1039/C8RA02557F
44. L.M. Tokubo, P.L. Rosalen, J. de Cássia Orlandi Sardi, I.A. Freires, M. Fujimaki, J.E. Umeda, P.M. Barbosa, G.O. Tecchio, N. Hioka, C.F. de Freitas and R.S. Suga Terada, *Photodiagn. Photodyn. Ther.*, **23**, 94 (2018); https://doi.org/10.1016/j.pdpdt.2018.05.004
45. C.M. Cassidy, R.F. Donnelly, J.S. Elborn, N.D. Magee and M.M. Tunney, *J. Photochem. Photobiol. B*, **106**, 95 (2012); https://doi.org/10.1016/j.jphotobiol.2011.10.010
46. S. Leonard, P. M. Gannett, Y. Rojanasakul, D. Schwegler-Berry, V. Castranova, V. Vallyathan and X. Shi, *J. Inorg. Biochem.*, **70**, 239 (1998); https://doi.org/10.1016/S0162-0134(98)10022-3
47. A. Hanakova, K. Bogdanova, K. Tomankova, K. Pizova, J. Malohlava, S. Binder, R. Bajgar, K. Langova, M. Kolar, J. Mosinger and H. Kolarova, *Microbiol. Res.*, **169**, 163 (2014); https://doi.org/10.1016/j.micres.2013.07.005
48. Z. Yaghobi, Z. Rashidi Ranjbar and S. Gharbi, *Polyhedron*, **164**, 176 (2019); https://doi.org/10.1016/j.poly.2019.02.039